A VERSATILE 3D CALIBRATION OBJECT FOR VARIOUS MICRO-RANGE MEASUREMENT METHODS

M. Ritter [a] *, M. Hemmleb [b], O. Sinram [b], J. Albertz [b] and H. Hohenberg [a]

[a] HPI, Electron Microscopy and Micro Technology Group, D-20251 Hamburg, Germany - (ritter, hohenberg)@hpi.uni-hamburg.de
[b] TU Berlin, Photogrammetry and Cartography, D-10623 Berlin, Germany - (hemmleb, sinram, albertz)@fpk.tu-berlin.de

Commission V, WG 1

KEY WORDS: Accuracy, Calibration, Close Range, Comparison, Correction, Microscopy, Orientation, Photogrammetry

ABSTRACT:

We present a new micrometer-sized 3D calibration structure containing nanomarkers that serve as well distinguishable reference points for the calibration of various 3D micro-range measurement methods, e.g. scanning electron microscopy (SEM) and environmental SEM (ESEM). The 3D calibration object was fabricated using gas-assisted focused ion beam (FIB) metal deposition. This technique proved to be a valuable tool, as it principally allows the construction of variously shaped microstructures that can be perfectly adapted to the special specifications of the sensor to be calibrated. The spatial data of the 38 non-symmetrically distributed nanomarkers were obtained by high-precision atomic force microscopy (AFM). The accuracy of the nanomarker measurement is shown and the efficiency of the calibration is demonstrated by triangulation and spatial intersection. Additionally, alternative micro-range measurement methods, e.g. confocal laser scanning microscopy (CLSM) and scanning profilometry were tested for possible application of the calibration structure.

1. INTRODUCTION

The importance and number of micro- and nano-technological applications in material science and in life science is rapidly increasing. The 3D analysis of microstructures generated by micro-fabrication as well as the spatial characterization of surface details requires adequate sensors and micro-range measurement methods. In general, all measurement processes are subdivided into contact and non-contact methods. Whereas most close range measurements work with tactile mechanisms or use light waves as information carriers, a variety of methods have been developed for non-contact micro-range measurements. An overview of relevant 3D micro-range measurement methods will be given in chapter 2.

A most suitable sensor is the electron microscope. Modern techniques in scanning electron microscopy like ESEM-technology offer the possibility of imaging even hydrated microstructures while maintaining their original 3D topography. The application of photogrammetric methods for the analysis of electron microscopic data has a long tradition and has become the method of choice for the quantitative 3D-reconstruction of SEM or (ESEM) images: SEM data provide a large depth of focus, a high signal to noise ratio and images can be captured over a wide range of magnification. The efficiency of the photogrammetric method has been proved in numerous applications e.g. the characterization of microstructures, the topographic analysis of frictions and the reconstruction of biological surfaces [König et al., 1987, Scherrer et al., 1999, Hemmleb et al., 2000, Hemmleb, 2001, Ritter et al., 2003].

However, quantitative photogrammetric reconstruction of electron microscopic data requires a set of basic components. We recently presented a micrometer-sized 3D calibration structure that allows the calibration of SEM [Sinram et al., 2002a]. Yet, also optical errors of alternative micro-range measurement methods, e.g. ESEM or confocal laser scanning microscopy (CLSM) and scanning profilometry can be detected. The 3D microstructure was fabricated using gas-assisted focused ion (FIB) beam technique. Based on this technique, an optimally designed 3D micro-object was created. The subsequent high precision spatial measuring with atomic force microscopy (AFM) made a calibration object out of the fabricated structure.

Here, we describe a method which makes it possible to build 3D structures of various size with a flexible design in order to fit specific applications. Multiple sensors could be calibrated and thus a comparative analysis of the quantitative microscopic data and their significance can be accomplished. Thus, we will give a short overview of 3D micro-range measurement methods connected to this work.

2. SENSORS AND METHODS FOR 3D MICRO RANGE MEASUREMENTS

2.1 Overview Micro-Range Measurement Methods

Non-destructive 3D micro-range measurement methods exist in a great variety. For the determination of material parameters, typically tactile methods are chosen. Optical measurement methods are used for 3D surface or volumetric measurements. Various optical measurement techniques were adapted to micro-range requirements. For higher resolutions, methods are needed, which overcome the borders of light microscopy. Using electrons for imaging, the determination of 3D information results from image processing methods, e.g. photogrammetric or tomographic algorithms. Electron beam imaging in combination with 3D image processing

* Corresponding author.

offers the possibility to bridge optical 3D measurement methods and scanning probe microscopy. For a better understanding, 3D measurement methods in micro-range are divided into surface und volumetric methods. An overview of important techniques is given in Table 1. The next two chapters will deal with an overview of relevant micro-range measurement methods.

Surface measurement methods	**Volumetric measurement methods**
Profilometry (optical or mechanical)	Light Microscopy and shape from focus
Micro-optical triangulation methods (structured light)	Confocal Laser Scanning Microscopy (CLSM)
(Environmental) Scanning Electron Microscopy ([E] SEM) combined with photogrammetry	Transmission Electron Microscopy (TEM) and tomographical methods
Atomic Force Microscopy (AFM)	Micro-Tomography (Micro CT)
(Laser-) Interferometry	

Table 1. 3D micro-measurement methods

2.2 Surface measurement

Scanning Electron Microscope and Photogrammetry

The electron microscope uses electrons instead of light for imaging. In scanning electron microscopy, the signal of a sample surface is generated by an accelerated electron beam that is scanned over a sample surface "line by line". Thereby, electrons of the primary beam interact with the atoms of the surface. In elastic and inelastic scattering processes, electrons of a broad energy spectrum are emitted from the sample surface. Two different types of emitted electrons are commonly used for imaging: Secondary (SE) and Backscattered (BSE) electrons. SE are created in the sample itself and only capable to leave it, if generated in the first few nanometres. Therefore, SE carry the high-resolution information. SE emitted from the sample are detected by a photomultiplier system. The signal is then converted to a digital grey-scale image with an analogue-digital-adapter.
What makes the SEM so valuable for micro-range measurements are the topographic details of the scanned images and the large depth of focus. Also, SEM provides a fairly high resolution due to the properties of the electron optical system. Although the wavelength of the electrons could be in the picometer range, due to lens aberration the aperture of the magnetic lenses of electron microscopes must not exceed values of about 10-2 rad (0.7 - 1.3 rad in light optics). This limitation results in a maximum resolution in the nanometer range. The depth of focus is also affected by the electron-probe aperture and is quite large in correspondence to the small aperture. The depth of focus of a SEM is at least 10 times the depth of focus of the LM. At high magnification it still is in the micrometer range. This fact had to be considered when planning size and shape of the calibration object.

A specific feature of image acquisition with the SEM is the formation of very long focal length in combination with a virtual projection centre. Therefore, the image process is described with parallel geometry. Magnification and working distance, which is the distance between the electron emission pole and the specimen, have to remain constant during image acquisition for photogrammetric evaluation. Photogrammetric processing software has to take into account the special properties of SEM imaging described above. In order to increase the accuracy of 3D point determination, a bundle adjustment with should be applied [Maune 1976, Ghosh et al., 1976, El Ghazali 1984, Hemmleb 2001]. At magnifications higher than 500, usually parallel projection equations are used. The bundle adjustment approach also offers the possibility for photogrammetric calibration of SEM. With the known calibration parameters of the SEM and defined rules for the image data acquisition, the photogrammetric processing of surface models requires mostly only two images. They have to be achieved by tilting the sample on a suitable working stage [Sinram et al., 2002b].

The calibration of SEM includes at least the determination of the particular magnification (image scale) and the tilting angles. Depending on the chosen imaging model, the focal length has to be calculated too. Because of the necessity to rotate the sample in a fixed imaging system (like the SEM) the calibration data describe the motion of the working stage. The calibration of the SEM should be repeated from time to time, because the conditions of image acquisition do not remain constant in electron microscopy.

Environmental Scanning Electron Microscope (ESEM) and Photogrammetry

A special kind of scanning electron microscopy technique that operates at high pressures was introduced 1979 by Danilatos [Danilatos et al., 1979]. On the one hand, the technique allowed to look at liquid and hydrated samples and it simplified the preparation of the specimen. The approach was optimized by FEI Company (Eindhoven, Netherlands) and is offered under the name "environmental scanning electron microscope" (ESEM). The ESEM operates at pressures of 0.1 to about 20 Torr in its specimen chamber. The minimum pressure to keep water in the liquid phase at 4°C is 6.1 Torr. A multiple pressure limiting aperture system (PLA) supplemented by a gaseous secondary electron (GSE) detector enables the ESEM to work under such conditions The PLA system allows a high water pressure in the specimen chamber without affecting the high vacuum at the top of the microscope column, where the electron source is located. It is not possible to use the regular SE detector in a gaseous environment. But, the GSE- detector takes advantage of the presence of gas in the specimen chamber where the SE scatter at the gas molecules present in the specimen chamber. One effect of the collision is the release of more SE from every collision, thereby provoking a cascade reaction with sufficient SE yield for the GSE detector. The ESEM is frequently used in material research, dental research and more and more in the field of life sciences.

Atomic Force Microscopy

Atomic Force Microscopy (AFM), also known as Scanning Force Microscopy (SFM) belongs to the methods of Scanning Probe Microscopy (SPM). The AFM measures atomic interactions between the sample surface and the probe head.

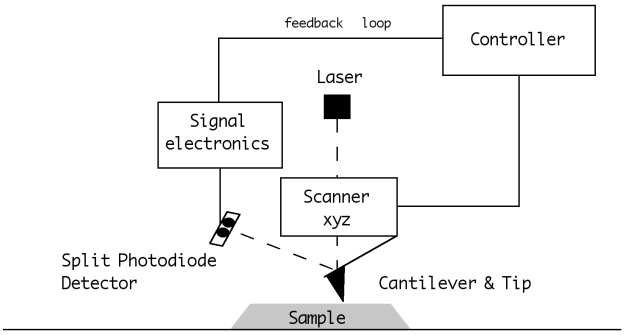

Figure 1. AFM contact and non-contact mode. In contact mode, the change of the cantilever deflection is monitored with the split photodiode detector. A feedback loop tries to keep the cantilever deflection constant by moving the z-scanner in order to maintain a constant photodetector difference signal. The topographic information is related to this movement of the z-scanner. When in non-contact mode, the scanning tip oscillates close to the sample surface. Here the oscillation amplitude is kept constant and used for topographic information.

The probe head is a tip mounted on the top of a flexible cantilever (Figure 1), which scans across the sample surface. For high resolution, the tip has to be very sharp, usually between 2nm to 20nm. A piezoelectric tube scanner performs the scan. Thereby, either the tip is moved or the sample itself, depending on the device used. The tip surface interaction is monitored by the reflection of a laser beam at the cantilever. The laser is detected by a split photodetector, where the difference in the photodetector output voltage is related to either the cantilever deflection or the oscillation amplitude.
In order to use scanning probe methods for the spatial measurement of surfaces, the measured values (Current) have to be transformed into metric measures. This involves special complications, because of the non-linearity of the scanning motion and the measurement errors due to the complex probe and sample geometry, which are hard to determine. A solution of this problem is provided by the development of metrological AFM (MAFM). These combine a high vertical measuring accuracy of AFM with the exact lateral measuring, for instance by controlling the motion of the AFM with interferometric methods. Because of the combination of several sophisticated instruments, these devices are custom-made and therefore very expensive. They are used mainly for calibration purposes.

2.3 Volumetric measurement

Confocal Laser Scanning Microscopy

Confocal Laser Scanning Microscopy (CLSM) is a 3D light microscopy technique. The CLSM is based on conventional microscopes, but the light source is a laser. The laser beam is focused on a sample in a way, that only one object point is illuminated. A detector pinhole discriminates against scattered light that is not emitted in the plane of focus. The resulting signal information from every object point represents a data cube. The CLSM can be used in reflection mode to characterize topographies. In order to achieve higher resolutions, a laser beam is applied in combination with a 3D scanner. The resolution of a CLSM is then restricted by the wavelength of the used laser and the resolution of the scanning system. CLSM images can be acquired of a wide range of samples, if only the minimum requirements concerning reflection are fulfilled. But, since most objects do not behave as perfect mirrors, data from reflection mode have to be carefully interpreted. The use of CLSM in life science is well established for a broad range of research activities [see Pawley, 1990], whereas the application in technical and material science is rather new [Wendt, 1995, Tiziani et al., 2000].

3. A VERSATILE CALIBRATION OBJECT

In the first place, it has been our aim to create a method for the quantitative 3D reconstruction of SEM data. This task could be achieved by using an appropriate tilting stage and a suitable calibration object [Sinram et al., 2002b]. But, more and more it became clear that there is a general wish to combine existing data with additional specific information provided only by other micro-range measurement methods. The correlation of complementary information from samples of interest offers new characteristics and a more precise analysis of surface features, e.g. if scanning electron microscopy and confocal laser scanning microscopy are combined [Al Nawas et al., 2001, Wessel et al., 2003]. Yet, in order to be able to correlate additional data with existing 3D datasets, the accuracy of all methods involved has to be determined. To us, the easiest and most accurate way to accomplish this task is the calibration of all the micro-measurement methods involved with one calibration object.
Since every sensor used for analytic purposes has its specific optical and mechanical peculiarities, the calibration object has to be carefully designed in order to cope with a variety of requirements. Most important was the decision to use gas assisted focused ion beam (FIB) metal deposition to produce the 3D micro-object. This method allowed the fabrication of 3D objects of various shape and structure. However, the precision to be achieved with this kind of technique has its limits and up to now, can only be roughly estimated. Considering all of the above facts, we found a possibility, which is not simply a compromise but a new methodological approach. It allows correlative 3D microscopy by using a flexible calibration technique.

3.1 Fabrication by gas assisted ion beam deposition

The most suitable way for the fabrication of the calibration object was found in the technique of gas assisted focused ion beam deposition [see Steckl et al., 1988]. Focused ion beam (FIB) systems operate similar to scanning electron microscopes, though a focused beam of gallium ions (Ga^+) instead of an electron beam is used. The FIB technique allows imaging or patterning of structures. Patterning in this case either means the process of specific removal of material as the beam scans along the sample surface, or the process of specific deposition of metal (by gas assisted deposition) onto the surface (Figure 3).
When the gallium ions of the primary beam hit the sample surface, a small amount of material is sputtered, leaving the surface as either ions or neutral atoms. This process is called milling. Additionally, the primary beam produces secondary electrons (SE). The secondary electrons can be used for imaging or for gas assisted deposition. If an organometallic gas, e.g. $W(CO)_6$ is introduced into the sample chamber of the microscope, it interacts with the secondary electrons of the ion beam as well as the beam itself and forms a non-volatile product that adsorbs on the surface. Lateral deposition and structure formation can be controlled by

blanking and unblanking the beam at specific lateral coordinates (Figure 2). Repetitive scanning of the ion beam in presence of the gas then results in the construction of a multilayer metal film of determined height and form, in our case the slope step pyramidal structures.

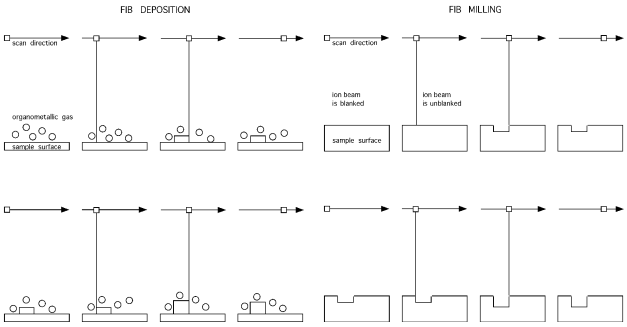

Figure 2. Schematic drawing of the two patterning modes of focused ion beam (FIB) systems. In the left drawing, the process of milling is shown. In the right drawing, the process of deposition is shown. The deposition product is a layer of metal, usually tungsten (W) or platinum (Pt). The metal is introduced into the specimen chamber as an organometallic compound. It is applied very close to the sample surface through a valve needle with a very fine tip. If hit by the ion beam or the secondary electrons generated by the beam at the sample surface, the organometallic gas decomposes, whereby the metal deposits at the sample surface.

3.2 Design and specification

The development and design of the calibration object was determined by the various demands of the particular measurement methods (Figure 3).

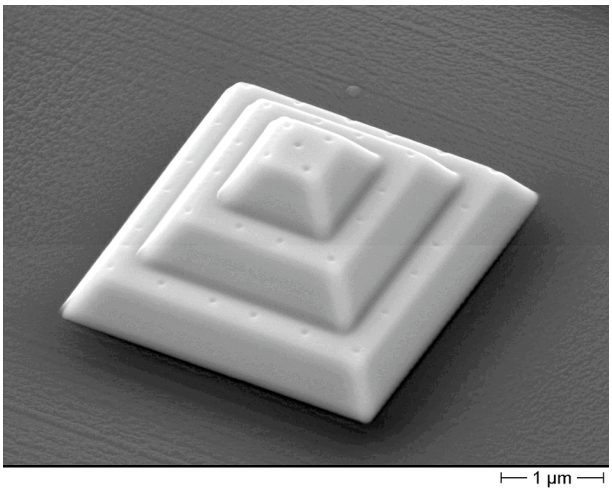

Figure 3. SEM image of a calibration pyramid made with the technique of gas assisted FIB. The pyramidal shaped calibration object with slope steps approximately measures 6µm in width and length and 3µm in height. It can be used for SEM calibration at magnifications of 8000x to approx. 20000x. The calibration object has up to 38 nanomarkers as control points. They were applied using FIB milling. The distribution of the nanomarkers is non-symmetrical, so they can always be clearly identified and associated.

Also, the peculiarities of the calibration process itself had to be taken into consideration. In general, it is an advantage in 3D measurement methods, if the calibration object covers the measurement volume. This is especially important in 3D measurements with SEM, because the positioning of the calibration object is restricted by the properties of the sample and the tilting stage.

Nanomarkers [Hemmleb et al., 1995, Sinram et al., 2002b] on the calibration object serve as control points carrying the spatial information. They must be easy to detect as discrete points in both, the scanning electron microscope and the atomic force microscope. The distribution on the lower level is non-symmetrical, in order to be always informed of the pyramid's orientation. The control points are detected via semi-automated image processing methods. Therefore, their coordinates can be directly used for the photogrammetric bundle block adjustment. The cascade pyramidal shape of the calibration structure allows the usage at a range of magnifications. Together with the sloping edges, it is guaranteed that the control points on a lower level maintain visible, even if tilted in the SEM for the calibration process. Additionally, the angle of the pyramidal cascade step slopes, in respect to the surface plane was designed to be smaller than the aperture angle of the AFM tip.
We wanted to be able to calibrate the SEM at a maximum range of magnification. Therefore, the measures had to represent a structure that is still completely within the range of the depth of focus, when filling the field of view of an SEM image. Most AFM scanners can handle a scan area up to 100µm with a maximum structure elevation of about 8µm. Therefore the size of the calibration structure was limited by the specifications of the AFM scanner and the optical limitations of the SEM.

3.3 Application for correlative measurements

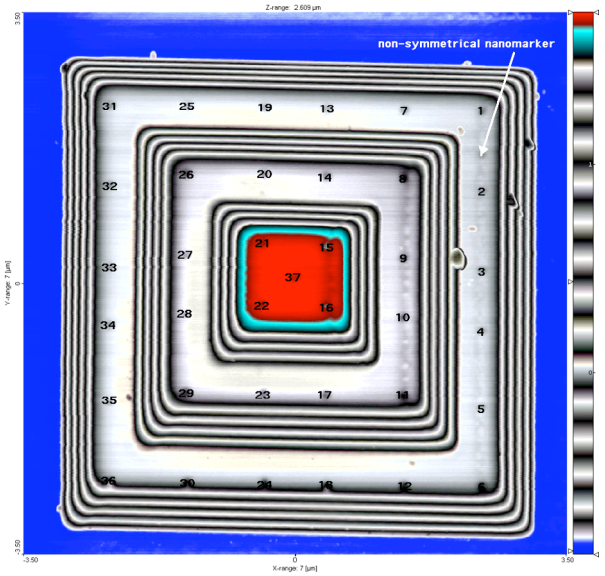

Figure 4. Contour plot of the calibration object measured by atomic force microscopy at the PTB (Phsikalisch-technische Bundesanstalt, Braunschweig). Nanomarkers are marked as numbers 1 to 37. The arrow shows the symmetry breaking nanomarker.

Figure 3 and Figure 4 show the functionality of the design of the 3D pyramidal calibration object, because the nanomarkers can be clearly identified in both measurement

methods. Additionally, the pyramidal structure can be tilted in the SEM for calibration purposes with still all of nanomarkers visible to the electron beam. Also, due to the slope steps of the calibration object, AFM measurements are possible and provide the spatial information of the reference points that is needed for the calibration of scanning electron microscopes.

4. MEASUREMENT RESULTS

4.1 AFM measurement results

High precision AFM measurements in non-contact mode were done at the PTB (Physikalisch-Technische Bundesanstalt, Braunschweig, Germany). The instrument used was a modificated SIS-AFM Nanostation III (SIS, Herzogenrath, Germany) with strain gauges in z-direction and lateral capacitive sensors to guarantee lateral high-precision measurements. Although the device is not approved for metrological measurements, results within 1% of uncertainty in z-direction can be expected.
Alternatively, the nanomarker coordinates were measured with a "normal", commercially available Veeco Explorer 2000 (Veeco, Woodburry, USA) AFM in contact mode.
Nanomarker coordinates of all measurements were detected using a geometric search routine, sensitive to sudden changes in altitude on smooth topographies. Then, the high precision SIS-AFM data were compared with the raw and corrected data of the Explorer AFM (Table 2 and Figure 5). Determination of the coordinates of the nanomarkers depends on the accuracy of the sensor as well as on the accuracy of the analysis used. From the analysis, a lateral mean point error of 0.9 Pixel has been evaluated, corresponding to a relative error of 0.0009 in a 1000 pixel scan. The relative vertical error is about 0.002. Therefore, the sensor is the limiting factor. This can be clearly seen, when comparing the accuracy of the high-precision SIS-AFM with a commercially available AFM, e.g. the Veeco Explorer we used in our first approaches for reference point determination. Further improvements will be possible by measuring with an interferometrically controlled, metrological AFM (MAFM).

AFM Sensor	S_A = relative Sensor Accuracy			rel. S_A + Nanomarker determination error		
	Δx	Δy	Δz	m_x	m_y	m_z
SIS	$5*10^{-4}$	0.006	0.01	$7*10^{-4}$	0.006	0.01
Veeco	0.1	0.3	0.06	0.1	0.3	0.06
Veeco calibrated	0.013	0.026	0.05	0.013	0.026	0.05

Table 2. The accuracy of the AFM measurements and nanomarker detection.

5. CALIBRATION RESULTS

With the nanomarker coordinates determined by high-precision AFM, we were able to calibrate a high-resolution field-emission SEM, the XL30 FEG as well as a XL30 ESEM under "wet mode" (1 Torr water vapour pressure) conditions. Calibration of the XL30 FEG was performed with 10 images tilted by steps of 5 degrees. Calibration of the XL30 ESEM was done with 5 images and arbitrary tilt steps. Tables 3 and 4 show the calibrated magnification factor (m), the mean lateral (m_{X0}, m_{Y0}) and the mean tilt angle error calculated ($m\alpha$, $m\beta$, $m\gamma$).

5.1 SEM calibration results

Sensor	XL30 FEG
scale (m)	0.094 [pixel/nm]
mean (m_{X0}, m_{Y0}) [nm]	13.03, 13.15 [nm]
mean ($m\alpha$, $m\beta$, $m\gamma$)	0.781, 0.804, 0.248 [deg]

Table 3. Calibration results of the XL30 FEG scanning electron microscope.

5.2 ESEM calibration results

Sensor	XL30 ESEM
scale (m)	0.1133 [pixel/nm]
mean (m_{X0}, m_{Y0})	10.228, 10.075[nm]
mean ($m\alpha$, $m\beta$, $m\gamma$)	0.643, 0.654, 0.18 [deg]

Table 4. Calibration results of the XL30 ESEM scanning electron microscope.

5.3 Spatial intersection and triangulation

Results of the XL30 FEG calibration were tested by applying spatial intersection or triangulation formulas to the nanomarker image coordinates.

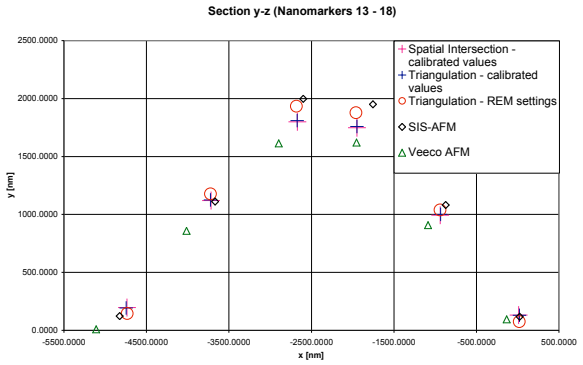

Figure 5. Section in y-z of nanomarkers 13-18 from AFM measurements and from applying spatial intersection or triangulation formulas.

The nanomarker coordinates in Figure 5 were calculated either from the calibrated values or from the microscope and tilting stage settings. Spatial nanomarker data from SIS-AFM and Veeco AFM are shown for comparison. In lateral direction, we found a good match of the calculated coordinates of the REM data with the AFM measurement. However, in vertical direction errors up to 5% did occur. Comparison of SIS-AFM and Explorer AFM data showed great discrepancy, even with calibrated Explorer data. Therefore, the importance of using high-precision AFM for accurate 3D micro-measurements is clearly underlined.

5.4 Correlative investigations

The calibration object has been tested preliminarily for other 3D micro-measurement methods, e.g. CLSM (Leica, Bensheim, Germany) and laser profilometry (Nanofokus, Oberhausen, Germany). Resolution of both measurement methods is insufficient to visualize the nanomarkers, but profile plots of the CLSM and profilometer measurements were compared to the original high-precision AFM measurement (Figure 6).

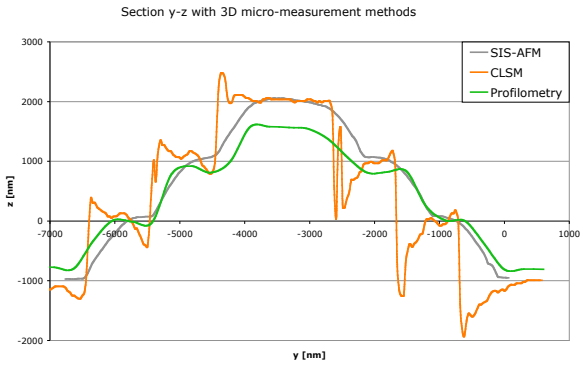

Figure 6. Profile plot of the calibration object by correlative 3D micro-range measurement methods: AFM (grey), CLSM (orange), profilometer (green).

While lateral and vertical analysis of the reflection mode CLSM measurements do fit quite well, the reflection artefacts of the measurement method at the pyramids edges can be clearly seen. Lateral laser profilometry results are in good agreement to the AFM reference. Though, in vertical direction, a discrepancy of about 10% in height can be stated. The reason for this difference is not yet clear and has to be further investigated.

6. DISCUSSION AND OUTLOOK

With a new versatile calibration object we have been able to calibrate scanning electron microscopes at high magnification within certain limits of accuracy. The results are very promising and the calibration object and the method will be further optimized. Additionally, it should be possible to apply the 3D micro-object for calibration of confocal light scanning microscopes. The nanomarker radius could be altered, so that the reference points lie within the resolution limits. Eventually, a bigger gap between the single pyramidal steps will prevent scattering artefacts in the CLSM data.

7. REFERENCES

Al-Nawas, B., Grötz, K. A., Götz, H., Heinrich, G., Rippin, G., Stender, E., Duschner, H., Wagner, W., 2001. Validation of Three-Dimensional Surface Characterising Methods: Scanning Electron Microscopy and Confocal Laser Scanning Microscopy. *Scanning*, 23, pp. 227-231.

Danilatos, G.D., Robinson, V.N.E., 1979. Principles of scanning electron microscopy at high pressures. Scanning, 2, pp. 72-82.

El Ghazali, M., 1984. System Calibration of Scanning Electron Microscopes. International Archives of Photogrammetry and Remote Sensing 1984, Commission V, Vol. XXV, Part A5, pp. 258-266.

Ghosh S., Nagarja, H., 1976. Scanning Electron Micrography and Photogrammetry. *Photogrammetric Engineering and Remote Sensing*, 42(5), pp. 649-657

Hemmleb, M., Albertz, J., Schubert, M., Gleichmann, A., Köhler, J. M. 1995. Photogrammetrische Bestimmung der Krümmung einer Mikrokantilever-Probe mittels Raster-elektronenmikroskop. *Beiträge zur elektronenmikroskopischen Direktabbildung und Analyse von Oberflächen*, Band 28, Leipzig, pp.65-72

Hemmleb, M., Albertz, J. 2000. Microtopography - The photogrammetric determination of friction surfaces. International *Archives of Photogrammetry and Remote Sensing*, Vol. XXXIII, Amsterdam.

Hemmleb, M., 2001. Photogrammetrische Auswertung elektronenmikroskopischer Bilddaten. Ph.D. Thesis, Technical University of Berlin.

Koenig, G., Nickel, W., Storl, J., Meyer, D., Stange, J., 1987. Digital Stereophotogrammetry for Processing SEM Data. *Scanning*, 9, pp. 185-193.

Maune, D. F., 1976. Photogrammetric Self-Calibration of Scanning Electron Microscopes. *Photogrammetric Engineering and Remote Sensing*, 42(9), pp. 1161-1172.

Pawley J.B., 1990. *Handbook of biological confocal microscopy*, Chapter 2,11,14,17, Plenum Press, New York.

Reimer, L., 1998. *Scanning Electron Microscopy*. Springer, Berlin/Heidelberg/New York, Tokio.

Ritter, M., Sinram, O., Albertz, J., Hohenberg, H., 2003. Quantitative 3D Reconstruction of Biological Surfaces. *Microscopy and Microanalysis*, Vol. 9 (Suppl. 3), p. 476. Microscopy Conference MC 2003, Dresden, Germany.

Scherrer , S., Werth, P., Pinz, A., Tastschl, A., Kolednik, O., 1999. Automatic surface reconstruction using SEM images based on a new computer vision approach. *Electron Microscopy and Analysis*, 161, pp. 107-110.

Sinram, O., Ritter, M., Kleindiek, S., Schertel, A., Hohenberg, H., Albertz, J., 2002a. Calibration of an SEM, Using a Nano Positioning Tilting Table and a microscopic calibration pyramid. *International Archives of Photogrammetry and Remote Sensing*, Vol. XXXIV, part 5, pp. 210-216, ISPRS Commission V Symposium Corfu, Greece.

Sinram, O., Ritter, M., Schertel, A., Hohenberg, H., Albertz, J., 2002b. Ein neues Kalibrierobjekt für die Elektronenmikrophotogrammetrie. *Photogrammetrie–Fernerkundung-Geoinformation*, Heft 6, pp. 435-441.

Steckl, A.J., Corelli, J.C., McDonald, J.F., 1988. Focused Ion Beam Technology and Applications. In: *Emerging Technologies for In-Situ Processing*, eds. D.J. Ehrlich and V.Tran Nguyen, (NATO ASI Series, M. Nijhoff Publishers), pp. 179-199.

Tiziani, H.J., Wegner, M., Steudle, D., 2000. Confocal Principle for macro- and microscopic surface and defect analysis. *Optical Engineering*, 39(1), pp. 32-29.

Wendt, U., 1995. Konfokale Laserrastermikroskopie zur Quantifizierung von Bruchflächen. *Beitr. Elektronenmikr. Direktabb. Oberfl.*, 28, pp.37-42.

Wessel, S., Pagel, S., Ritter, M., Hohenberg, H., Wepf, R., 2003. Topographic Measurements of Real Surface in reflection Confocal Laser Scanning Microscopy (CLSM). *Microscopy and Microanalysis*, Vol. 9 (Suppl. 3), p. 162. Microscopy Conference MC 2003, Dresden, Germany.

8. ACKNOWLEDGMENTS

We kindly want to acknowledge the help from Dipl.-Ing. Thorsten Dziomba Dr. Ludger Koenders, Pysikalisch-technische Bundesanstalt, Braunschweig, Germany for high-precision AFM measurements and fruitful discussions. We also want to thank Dr. Roger Wepf, Dr. Sonja Wessel, and Sonja Pagel, Analytical Microscopy, Beiersdorf AG, Hamburg, Germany for CLSM (Leica, Bensheim, Germany) and Profilometer (Nanofokus. Oberhausen, Germany) measurement and FEI, Eindhoven, Netherlands for FIB time.